Title

Factors Determining the Superior Performance of Lipid/DNA/Protammine Nanoparticles over Lipoplexes

Journal

Journal of Medicinal Chemistry, 54(12)

ISSN

0022-2623

Authors

Caracciolo, Giulio

Pozzi, Daniela

Capriotti, Anna Laura

et al.

Publication Date

2011-06-23

DOI

10.1021/jm200237p

Journal of Medicinal Chemistry

ARTICLE

pubs.acs.org/jmc

Factors Determining the Superior Performance of Lipid/DNA/Protammine Nanoparticles over Lipoplexes

Giulio Caracciolo,[*,†] Daniela Pozzi,[†] Anna Laura Capriotti,[‡] Carlotta Marianecci,[§] Maria Carafa,[§] Cristina Marchini,[∥] Maura Montani,[∥] Augusto Amici,[∥] Heinz Amenitsch,[⊥] Michelle A. Digman,[#] Enrico Gratton,[#] Susana S. Sanchez,[#,∞] and Aldo Laganà[‡]

[†]Department of Molecular Medicine, "Sapienza" University of Rome, Viale Regina Elena, 324, 00161, Rome, Italy

[‡]Department of Chemistry, "Sapienza" University of Rome, P.le A. Moro 5, 00185 Rome, Italy

[§]Department of Drug Chemistry and Technologies, Faculty of Pharmacy, "Sapienza" University of Rome, P.le A. Moro 5, 00185 Rome, Italy

[∥]Department of Bioscience and Biotechnology, University of Camerino, Via Gentile III da Varano, 62032 Camerino (MC), Italy

[⊥]Institute of Biophysics and Nanosystems Research, Austrian Academy of Sciences, Schmiedelstrasse 6, A-8042 Graz, Austria

[#]Laboratory for Fluorescence Dynamics, Department of Biomedical Engineering, University of California, Irvine, 3120 Natural Sciences 2, Irvine, California 92697-2715, United States

[∞]Microscopy and Dynamic Imaging Unit, Centro Nacional de Investigaciones Cardiovasculares, Fundación CNIC-Carlos III, Madrid, Spain

Supporting Information

ABSTRACT: The utility of using a protammine/DNA complex coated with a lipid envelope made of cationic 1,2-dioleoyl-3-trimethylammonium propane (DOTAP) for transfecting CHO (Chinese hamster ovary cells), HEK293 (human embryonic kidney cells), NIH 3T3 (mouse embryonal cells), and A17 (murine cancer cells) cells was examined. The widely used DOTAP/DNA lipoplex was employed as a reference. In all the tested cell lines lipid/protamine/DNA (LPD) nanoparticles were more efficient in transfecting cells than lipoplexes even though the lipid composition of the lipid envelope was the same in both devices. Physical−chemical properties were found to control the ability of nanocarriers to release DNA upon interaction with cellular membranes. LPD complexes easily release their DNA payload, while lipoplexes remain largely intact and accumulate at the cell nucleus. Collectively, these data explain why LPD nanoparticles often exhibit superior performances compared to lipoplexes in trasfecting cells and represent a promising class of nanocarriers for gene delivery.

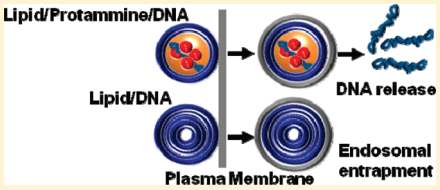

Gene therapy research is still problematic owing to a paucity of acceptable vector systems to deliver nucleic acids to patients for therapy.[1−3] Viral vectors are efficient but may be dangerous for routine clinical use. Synthetic nonviral vectors are fundamentally safer but are currently not efficient enough to be clinically viable. A possible solution for gene therapy lies with improved synthetic nonviral vectors based upon well-established platform technologies and a thorough understanding of the barriers to efficient gene delivery and expression (transfection) relevant to clinical applications of interest. One of the most common nonviral gene delivery vectors are DNA−cationic lipid complexes (lipoplexes). On the basis of freeze−fracture electron micrographs and X-ray diffraction studies, it was suggested that lipoplexes are multilamellar onion-like systems with DNA sandwiched between opposing lipid bilayers.[4−8] Once inside the cell, such multilamellar structure offers protection from DNA degradation but do not often allow for an adequate DNA release from endosomal compartments. If gene payload is not released from endosomes, it is shuttled to the lysosomes, where it is degraded by the abundant nucleases and transfection may fail.[9−11] To overcome this problem, lipid/DNA/polycation (LDP) complexes, in which plasmid DNA (pDNA) condensed with a polycation is encapsulated by a lipid envelope, have recently been developed.[12] Kogure et al.[12] demonstrated that the luciferase activity of a DNA−poly-L-lysine complex (DPC) with a lipid envelope was 10 times higher than only DPC in NIH 3T3 cells, suggesting that the lipid coating is important and critical for efficient gene delivery. Recent studies showed superiority of LPD-mediated gene transfer over conventional liposomes for delivering a gene to the liver.[13] Over the past few years several efforts to improve the delivery efficiency of LPD systems have been made.[14−18] The composition of the lipid envelope of LPD systems has been modified with novel chemical compounds, while the surface has been functionalized with several polymers and ligands. In a recent study a new lysine based cationic lipid containing a guanidine group that serves simultaneously as a delivery component and a therapeutic agent was reported.[16] Such

Received: March 1, 2011
Published: May 13, 2011

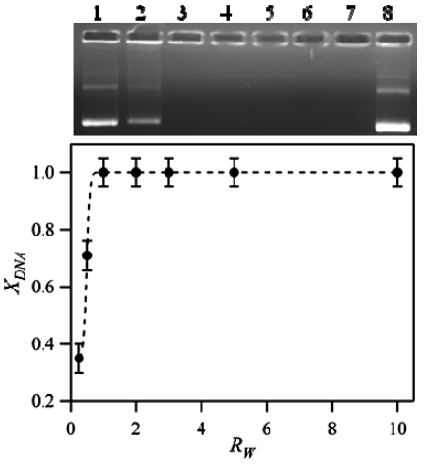

Figure 1. (Top) Digital photograph of protammine/DNA complexes (P/DNA) with increasing P/DNA weight ratio R_W: R_W = 0.1 (lane 1), R_W = 0.5 (lane 2), R_W = 1 (lane 3), R_W = 2 (lane 4), R_W = 3 (lane 5), R_W = 5 (lane 6), R_W = 10 (lane 7), and control DNA (lane 8). Experiments revealed two major bands for naked DNA (lane 8). The high-mobility band was attributed to the most compact (supercoiled) form, and the less-intense one was considered to be the non-super-coil content in the plasmid preparation. (Bottom) Molar fraction of plasmid DNA protected by protamine, X_{DNA}, against the P/DNA weight ratio, R_W.

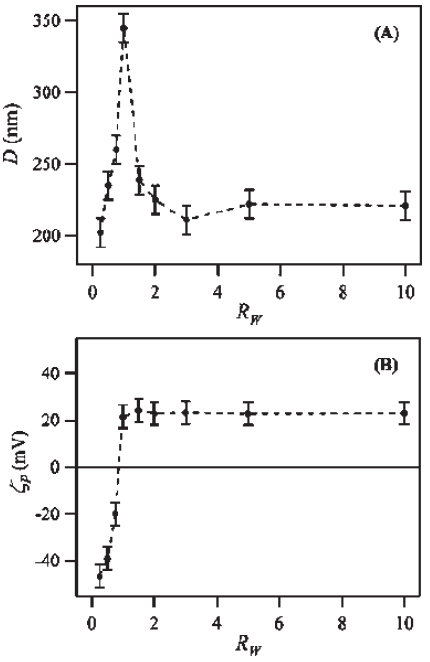

Figure 2. (A) Diameter of P/DNA complexes, D_H, as a function of the P/DNA weight ratio, R_W. This behavior is typical of the reentrant condensation effect. (B) ζ-Potential of P/DNA complexes as a function of R_W. The charge inversion effect occurring for 0.5< R_W <1 changes the overall charge of the aggregates from negative (DNA excess) to positive (protamine excess).

novel formulation resulted in enhanced cellular uptake, gene silencing, and tumor growth inhibition. Systemic tumor-targeted delivery remains the most challenging issue in the drug delivery field. In vivo data of tissue distribution demonstrated the potential of surface-modified LPD nanoparticles for tumor targeting.[15] Whether the superior performance of LPD systems over the consolidated lipoplex strategy does correlate with distinct physical−chemical properties of LPD complexes is an open question that needs to be answered. Generally, lipoplex dispersions are heterogeneous and polydisperse, consisting of a variety of structures in dynamic equilibrium. Recently, the existence of hybrid structures made of multilamellar lipoplexes stuck together by DNA has been reported.[19] Because physical−chemical properties of gene vectors may determine their interaction with cells and tissues, a precise knowledge of these properties may be important for predicting their biological response both in vitro and in vivo. Comparative studies of pDNA-encapsulation type and lipoplex type gene vectors would therefore provide useful information to decipher the relationship between the physical−chemical properties of gene vectors and their mechanisms of interaction with the cell's components. This knowledge is expected to drive the rational design of highly efficient gene delivery systems.

In the present study, we show that the transfection efficiency (TE) of protammine/DNA complexes coated with a lipid envelope made of cationic 1,2-dioleoyl-3-trimethylammonium propane (DOTAP) is from 3 to 20 times higher than that of DOTAP/DNA lipoplexes. We asked whether such remarkable difference in TE did correlate with particulate features of complexes. To answer this question, we investigated complex formation, DNA protection ability, surface properties, nanostructure, ability to release DNA upon interaction with cellular lipids, and intracellular trafficking. We present findings showing that the superior efficiency of LPD complexes over lipoplexes does correlate with their distinctive physical−chemical properties.

RESULTS

Complex Formation. Gel retardation assay was carried out to evaluate the condensing ability of P/DNA, LPD complexes, and lipoplexes.[20−24] The complete retardation of the binary P/DNA complex can be observed when the P/DNA weight ratio, R_W, was above 0.5 (Figure 1, top part). Starting from R_W = 0.75, the molar fraction of plasmid DNA completely protected by protamine, X_{DNA} (Figure 1, bottom part), was maximum (i.e., X_{DNA} = 1). P/DNAcomplex formation was investigated by measuring the average hydrodynamic radius, R_D, and the electrophoretic mobility of the diffusing complexes in the solution. The combined use of these two techniques allowed us to study both of the two typical phenomena occurring in these systems, namely, the reentrant condensation and the charge inversion effect.[25,26] In Figure 2 the average dimensions and the ζ-potential of P/DNA particles are plotted against R_W. As can be seen, with the increase in R_W, complex formation begins and the diameter of complexes, D_H, gradually increases until a maximum is reached at $R_W \approx 1$. Our results are in good agreement with previous studies showing that P/DNA particles show a neutral charge at R_W = 0.9.[27] Further increase in the P content determines the formation of decreasing-size complexes until the size of the original P/DNA core is approximately reached again (reentrant condensation). Aggregates also undergo the charge inversion effect, documented by the ζ-potential values whose sign changes for 0.5 < R_W <1, differentiating negatively and positively charged aggregates. On the basis of these results, P/DNA complex at R_W = 0.75 was therefore chosen because it guaranteed complete DNA protection, exhibited negative charge (−20 mV), and had appropriate dimensions (260 nm) with the minimum P content. Then the preassembled negatively charged P/DNA core was coated with a

dx.doi.org/10.1021/jm200237p |J. Med. Chem. 2011, 54, 4160–4171

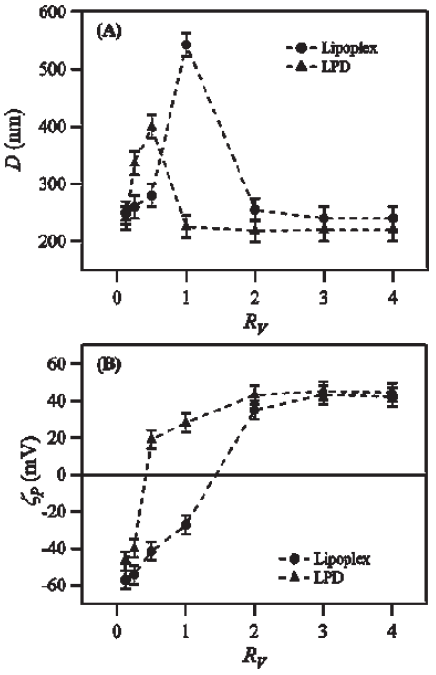

Figure 3. (A) Diameter of LPD complexes (triangles) and lipoplexes (circles) as a function of the lipid/DNA volume ratio, R_V. (B) ζ-Potential of LPD complexes (triangles) and lipoplexes (circles) as a function of R_V.

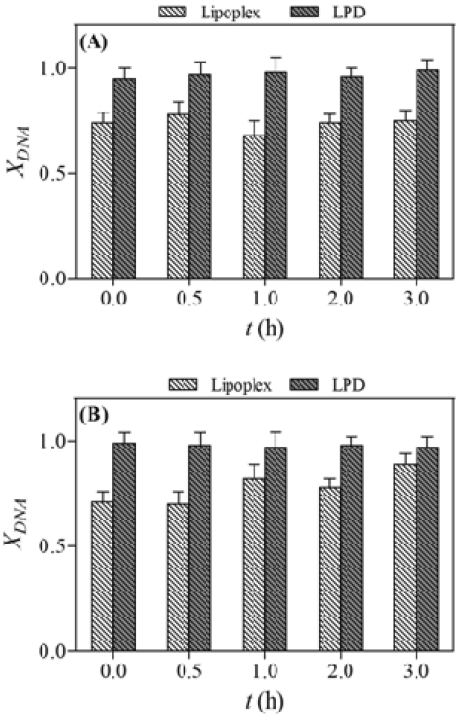

Figure 4. Molar fraction of DNA protected, X_{DNA}, by LPD nanoparticles and lipoplexes over incubation with buffer (A) and serum (B).

lipid envelope through membrane fusion of positively charged DOTAP small unilamellar vesicles (SUVs) (55 mV, R_H = 61.2 nm), triggered by the electrostatic attraction around the negatively charged core. The main results are summarized in Figure 3 where we show the diameter D_H (part A, triangles) and the ζ-potential ζ_p (part B, triangles) of DOTAP/P−DNA LPD complexes as a function of the lipid/DNA volume ratio, R_V. As can be seen, with the increase of R_V, complexation begins and the size of the complexes gradually increases until a maximum is reached ($D_H \approx 500$ nm at $R_V = 0.5$). Increasing the lipid content ($R_V > 0.5$) results in the formation of decreasing-size complexes. Aggregates also undergo the charge inversion effect, recognizable by the ζ-potential values (Figure 3b, triangles) whose sign changes around $R_V = 0.5$, differentiating negatively and positively charged aggregates. This trend shows three different ζ potential regions: (i) the region where the net charge of LPD complexes is negative and almost constant at (−31 mV); (ii) the region where the inversion of ζ potential sign takes place (around $R_V = 0.5$); and (iii) the region where the net charge of the LPD complexes is positive (47.8 mV). We observe that condensed P/DNA core (260 nm) is larger in size than the final LPD complex (~220 nm). This finding suggests that the P/DNA core is partly disassembled upon DNA−lipid interaction. Upon disassembling, some free DNA may give rise to a minor fraction of lipoplexes, if any, in the final dispersion. Even though the polydispersity index was low (pdi <0.25), this possibility cannot be excluded. In Figure 3 D_H (part A, circles) and ζ_p, (part B, circles) of DOTAP/DNA lipoplexes plotted against R_V are also reported. As evident, both the re-entrant condensation and the charge inversion effect occurred, but at R_V values larger than those observed in the case of LPD complexes. Dynamic investigation of size and ζ potential showed that both LPD nanoparticles and lipoplexes were fairly stable over 24 h (Supporting Information). The LPD complex at $R_V = 2$ was finally chosen because it exhibited positive charge (47.8 mV) as well as the lowest colloidal dimensions (220 nm) and the lowest polydispersity index (pdi = 0.22).

DNA condensation was also investigated by UV−vis absorption measurements by which the binding constants for both LPD complexes and lipoplexes were estimated ($K_{LPD} = (2.1 \pm 0.5) \times 10^4\ M^{-1}$ and $K_{Lipoplex} = (1.3 \pm 0.3) \times 10^4\ M^{-1}$; details are given in the Supporting Information). A slightly stronger lipid/DNA interaction for LPD systems was observed. Since the stability of lipid−DNA complexes is related to charge neutralization, our findings are most likely to indicate that protammine contributes to a better DNA charge neutralization.[28]

DNA Protection Ability. The DNA protection ability of both LPD nanoparticles and lipoplexes was investigated by electrophoresis on agarose gel. In Figure 4A we report the molar fraction of DNA protected by either lipoplexes and LPD nanoparticles, X_{DNA}, over the incubation period with cells. The starting point ($t = 0$) refers to the time when lipid vectors are usually given to cells, i.e., about 20 min of incubation after lipid−DNA mixing. At $t = 0$, the protection ability of LPD is almost complete while some free DNA is present in the lipoplex formulation ($X_{DNA} \approx 0.25$). Such values of protection remained the same over 3 h of incubation. The presence of serum in the transfection media has been found to be inhibitory to gene transfer.[29] This inhibition has been mainly attributed to serum−lipid membrane interaction resulting in destabilization of the lipid structure. Such structural degradation is often accompanied by lipid−DNA dissociation and release leading to a decrease in the DNA protection ability of complexes. We therefore investigated the protection ability of both LPD nanoparticles and lipoplexes in serum. As can be seen in Figure 4B, no relevant changes in the molar fraction of protected DNA, X_{DNA}, occurred. This indicates that the DNA-protection capacity of complexes was not modified by serum.

dx.doi.org/10.1021/jm200237p | J. Med. Chem. 2011, 54, 4160–4171

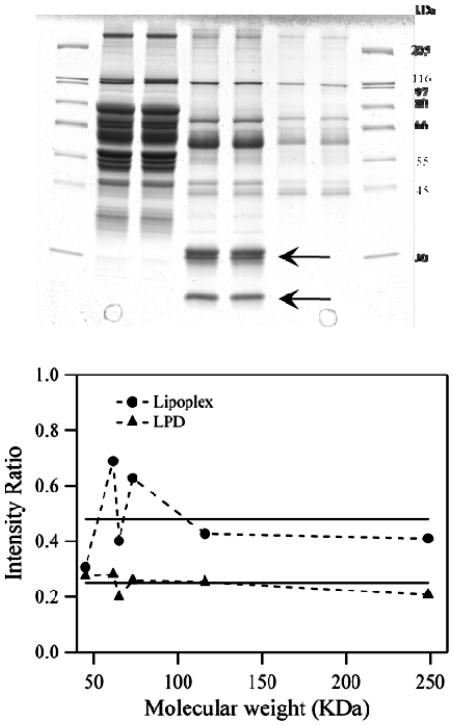

Figure 5. (Top) Photograph of an SDS−PAGE (12% gel) of human plasma proteins retrieved from DOTAP CLs (lanes 1 and 2), LPD complexes (lanes 3 and 4), and lipoplexes (lanes 5 and 6). Lane 7 is a protein molecular weight marker. The black arrows indicate the bands of human plasma proteins that were found to be much more abundantly associated with lipoplexes than with cationic liposomes. (Bottom) Intensity of protein band identified in the patterns of both lipid nanoparticles, I_{LPD}, and lipoplexes, $I_{Lipoplex}$, compared to the that of corresponding band identified in the patterns of DOTAP CLs, I_{DOTAP}. Intensity ratios (I_{LPD}/I_{DOTAP}, triangles) and ($I_{Lipoplex}/I_{DOTAP}$, circles) are plotted against the molecular weight of several protein bands, M_W. In the case of LPD complexes approximately uniform intensity ratios were observed, whereas intensity ratios of lipoplexes exhibited a random variation.

Surface Properties. Recent pioneering studies[30−34] have reported on the existence of a rich protein layer associated with the surface of nanoparticles after treatment with biological fluids (e.g., human plasma, HP). Here we perform proteomics experiments to investigate the "protein corona" associated with the surface of DOTAP cationic liposomes (CLs), LPD complexes, and lipoplexes after interaction with HP. Figure 5 (top part) shows one-dimensional sodium dodecyl sulfate−polyacrylamide gel electrophoresis (1D SDS−PAGE) (12% gels) of plasma proteins retrieved from DOTAP CLs (lanes 1 and 2), DOTAP/DNA lipoplexes (R_V = 2) (lanes 3 and 4), and LPD complexes (R_V =2) (lanes 5 and 6). As Figure 5 shows, 1D SDS−PAGE experiments were highly reproducible. Even though an accurate protein analysis is beyond the scope of the present study and will be given in detail elsewhere, some systematic effects were detected. We observe that the intensities of almost all protein bands of CLs (lanes 1 and 2) were higher than those of both lipoplexes (lanes 3 and 4) and lipid nanoparticles (lanes 5 and 6). Since the signal intensity within each scan is proportional to the vesicle surface available to plasma protein adsorption, this result indicates that the lipid membrane area of CLs that is available for binding is larger than that of lipoplexes and lipid nanoparticles.

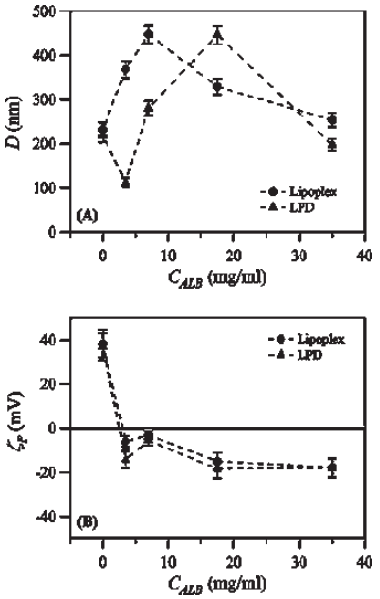

Figure 6. (A) Diameter of LPD complexes (triangles) and lipoplexes (circles) as a function of albumin concentration, C_{ALB}. (B) ζ-Potential of LPD complexes (triangles) and lipoplexes (circles) as a function of albumin concentration, C_{ALB}.

To find a surface similarity between the different surfaces, the intensity of each protein band identified in the patterns of both lipid nanoparticles, I_{LPD}, and lipoplexes, $I_{Lipoplex}$, was compared to that of the corresponding band identified in the patterns of DOTAP CLs, I_{DOTAP}. A comparative intensity analysis is reported in Figure 5 (bottom part) where the intensity ratios (I_{LPD}/I_{DOTAP}) and ($I_{Lipoplex}/I_{DOTAP}$) are plotted against the molecular weight of several protein bands, M_W. In the case of LPD complexes a series of approximately uniform intensity ratios was observed (Figure 5, bottom part, triangles). On the other hand, intensity ratios of lipoplexes (Figure 5, bottom part, circles) exhibited a random variation. This finding is most likely to suggest that the surface of LPD complexes has a high degree of similarity with that of pure DOTAP CLs, while that of lipoplexes has not. Furthermore, a protein band observed in the protein pattern of lipoplexes (indicated by black arrow in Figure 5, top part) was not detected in the pattern of CLs or in that of LPD nanoparticles. This high-intensity band was centered around 23 kDa. In this band a large number of Ig-Gs were identified by their mass (proteomics data not reported). Ig-Gs are basic proteins involved in many processes such as immunity response.[33] This finding indicates that the surface charge of lipoplexes differs, at least locally, from being positive. The latter observation is most likely to suggest that negatively charged DNA is adsorbed at the lipoplex surface and can interact with basic plasma proteins. In summary, our findings suggest that (i) the surface area of LPD complexes available to protein adsorption resembles that of DOTAP CLs (i.e., it is mainly lipidic) but it is smaller than that of pure DOTAP SUVs; (ii) the surface of lipoplexes is partly decorated with DNA molecules, while that of LPD is not.

We therefore asked ourselves whether the observed differences in the surface properties of lipoplexes and LPD nanoparticles may also affect their size and ζ-potential upon interaction with plasma proteins. To model the interaction of complexes with plasma proteins, albumin from bovine serum

dx.doi.org/10.1021/jm200237p |J. Med. Chem. 2011, 54, 4160–4171

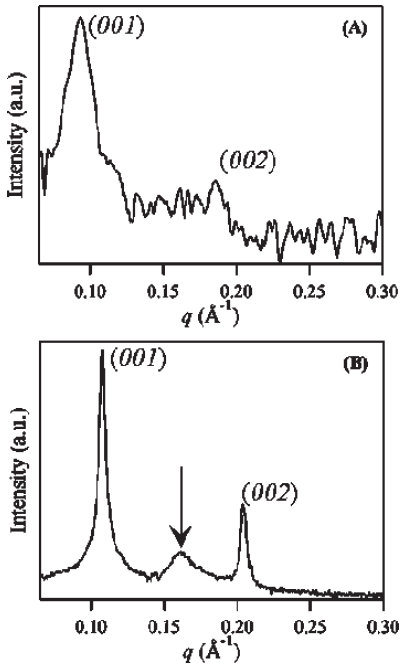

Figure 7. (A) Synchrotron SAXS pattern of LPD complexes at a lipid/DNA volume ratio, $R_V = 2$. Two broad Bragg peaks, corresponding to a periodicity $d = 2\pi/q_{001} = 7.10$ nm, were detected and larger than those commonly observed in most DOTAP/DNA complexes (typically 5.5−6.2 nm). (B) Synchrotron SAXS pattern of DOTAP/DNA lipoplexes ($R_V = 2$). The sharp periodically spaced peaks at q_{001} are caused by alternating lipid bilayer−DNA−monolayer structure with periodicity $d = 2\pi/q_{001} = 6.01 \pm 0.01$ nm. The middle peak (marked by an arrow) results from one-dimensional (1D) ordering of the DNA sandwiched between the lipid bilayers and corresponds to a DNA interhelical spacing $d_{DNA} = 2\pi/q_{DNA} = 4.01$ nm.

(Sigma-Aldrich, St. Louis, MO) was employed. Albumin is the main protein of HP and is negatively charged at physiological pH. Size and ζ-potential of complexes were investigated as a function of increasing albumin concentration, C_{ALB}, from zero up to its typical concentration in plasma (35 mg/mL). Figure 6A shows that upon interaction with albumin, the size of both lipoplexes and LPD nanoparticles increased with increasing albumin concentration, passed throughout a maximum, and finally reached a plateau value. On the other side, the ζ potential (Figure 6B) changed from positive (∼40 mV) to negative values (about −20 mV). Even though albumin changed the ζ-potential of lipoplexes and LPD nanoparticles to negative, gel electrophoresis showed that albumin was never able to release pDNA from the complexes (data not shown). Such finding is in very good agreement with the results of Figure 4B showing that the DNA protection ability of complexes is not affected by serum.

Nanostructure. Figure 7A shows the synchrotron SAXS pattern of LPD complexes ($R_V = 2$). As evident, two broad Bragg peaks, corresponding to a periodicity $d = 2\pi/q_{001} = 7.10$ nm, were detected. The large peak width, which is characteristic of a system with a short scattering correlation length, is an indication that the bilayers are weakly bound. Further, the lamellar periodicity, d, is larger than that commonly observed in most DOTAP/DNA complexes (typically 5.5−6.2 nm).[4−7] This suggests that the lipid membranes are in a highly swollen state due to electrostatic repulsion between adjacent charged DOTAP bilayers. From the full width at half-maximum (fwhm) of the

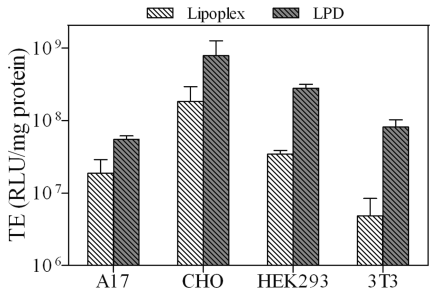

Figure 8. Transfection efficiency of LPD complexes and lipoplexes at the same lipid/DNA ratio ($R_V = 2$). Luciferase activity is expressed as relative light units/mg of protein in the cell lysate.

first-order lamellar Bragg peaks, a domain lamellar size of $L_m = 2\pi/\text{fwhm} \approx 70$ nm could be estimated. These observations are consistent with a model of LPD complexes made of a P/DNA core coated with a lipid envelope made of about 10 DOTAP bilayers.

We next examined the nanostructure of DOTAP/DNA lipoplexes. Figure 5, top, shows the SAXS pattern of DOTAP/DNA lipoplexes ($R_V = 2$). The sharp periodically spaced peaks at q_{001} are caused by alternating lipid bilayer−DNA−monolayer structure with periodicity $d = 2\pi/q_{001} = 6.01 \pm 0.01$ nm. This result is in agreement with previous experimental evidence of the DNA-induced liposome restructuring upon lipoplex formation provided by different techniques such as X-ray diffraction and cryoelectron microscopy.[4−8] The middle peak (marked by an arrow) results from one-dimensional (1D) ordering of the DNA sandwiched between the lipid bilayers.[23,24] It is usually referred to as "DNA peak" and corresponds to a DNA interhelical spacing $d_{DNA} = 2\pi/q_{DNA} = 4.01$ nm. From the fwhm of the first-order lamellar Bragg peaks, a domain lamellar size of about $L_m = 2\pi/\text{fwhm} \approx 200$ nm could be estimated. Given the lamellar d-spacing, $d = 6.00$ nm, this finding suggests that DOTAP/DNA lipoplexes are multilamellar onion-like structures made of more than 30 repeating lipid bilayer/DNA monolayer repeat units.[4−8]

Transfection Efficiency. To compare the ability of LPD nanoparticles and lipoplexes ($R_V = 2$) to deliver plasmid DNA, TE experiments were performed in NIH 3T3, CHO, Hek293, and A17 cells. TE results are reported in Figure 8. According to the literature, TE was found to be dependent on the given cell line. The CHO cell line was much more easily transfected than the A17 one, while intermediate levels of transfection were obtained with Hek 293 NIH 3T3 and cells. Even though different cell lines exhibited varying levels of TE, Figure 8 clearly shows the superior performance of LPD nanoparticles over lipoplexes in all the tested cell lines. TE was found to increase by a factor of ∼3 in A17, ∼4 in CHO, ∼8 in Hek293, and ∼20 in NIH 3T3 cells.

Interaction with Cellular Lipids. A viewpoint now emerging is that a critical factor in the lipid-mediated gene delivery is the structural evolution of lipoplexes upon interaction and mixing with anionic cellular lipids.[20,21,35−38] Such a structural rearrangement is supposed to play a central role in the DNA escape process, i.e., in how DNA dissociates from lipoplexes and is released into the cytoplasm and eventually into the nucleus. Thus, we were particularly interested in whether the DNA release from complexes upon interaction with cellular lipids might correlate with the TE data reported in Figure 8. Electrophoretic experiments (digital photographs not reported for space consideration) allowed us to quantify the molar fraction of DNA that

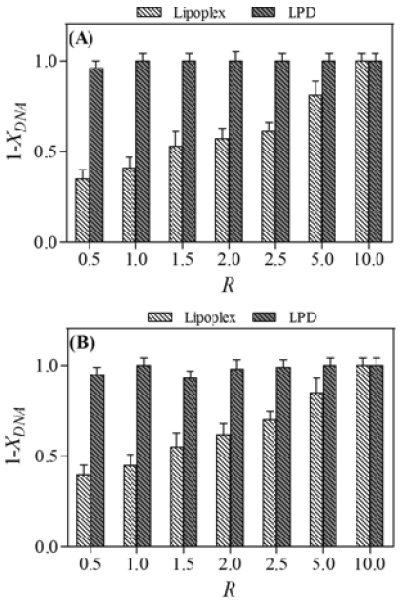

Figure 9. Molar fraction of DNA, $1 - X_{DNA}$, that is no longer electrostatically associated with LPD complexes and lipoplexes after interaction with DOPG (A) and DOPA (B) cellular lipids of as a function of the anionic/cationic charge ratio, *R*.

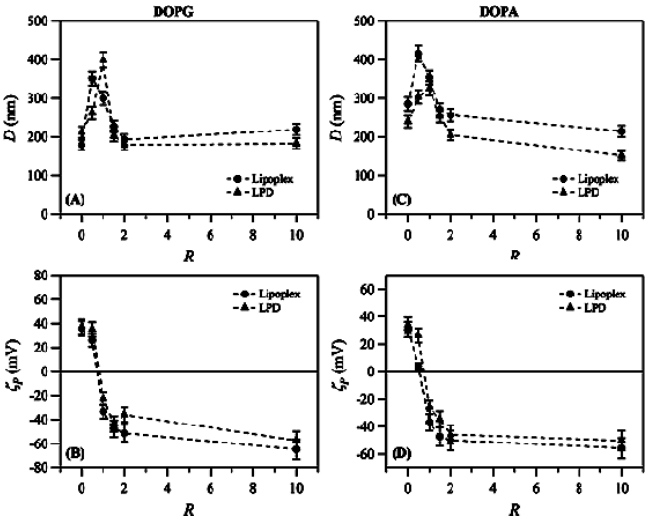

Figure 10. (A) Diameter of LPD complexes (triangles) and lipoplexes (circles) upon interaction with DOPG as a function of the anionic/cationic charge ratio, *R*. (B) ζ-Potential of LPD complexes (triangles) and lipoplexes (circles) upon interaction with DOPG as a function of the anionic/cationic charge ratio, *R*. (C) Diameter of LPD complexes (triangles) and lipoplexes (circles) upon interaction with DOPA as a function of the anionic/cationic charge ratio, *R*. (D) ζ-Potential of LPD complexes (triangles) and lipoplexes (circles) upon interaction with DOPG as a function of the anionic/cationic charge ratio, *R*.

is no longer electrostatically associated with cationic lipids, $1 - X_{DNA}$, as a function of the anionic/cationic charge ratio *R* upon interaction with DOPG (Figure 9A) and DOPA (Figure 9B) cellular lipids. At the lowest *R* ($R = 0.5$), DNA is almost completely dissociated from LPD complexes ($1 - X_{DNA} \approx 1$), while a large fraction of DNA is still protected by lipoplexes ($1 - X_{DNA}$ of ~0.35 and ~0.45 for DOPG and DOPA, respectively). Figure 9 also shows that DNA released from lipoplexes, $1 - X_{DNA}$, increases with increasing *R* and reaches 1 at $R \approx 10$. These findings suggest that a much lower amount of anionic lipids (ALs) is needed to promote complete DNA dissociation from LPD complexes.

Size and ζ-potential of lipoplexes and LPD nanoparticles upon interaction with cellular lipids are reported in Figure 10. Addition of ALs to cationic complexes results in a marked increase in size until a maximum is reached (at *R* of ~0.5 and ~1 for lipoplexes and LPD systems, respectively). Upon further addition of anionic charge, vesicle size reverted to control values. The observed increase in size of complexes for $R < 1$ can be either associated with van der Waals attractions overcoming weak electrostatic repulsions (reentrant condensation) or to vesicle fusion. Aggregates also undergo the charge inversion effect, documented by the ζ-potential values whose sign changes for $0.5 < R < 1$, differentiating positively and negatively charged aggregates. Size and ζ-potential of complexes after interaction with ALs were pretty stable over 24 h (data not reported for space consideration). On the basis of the analysis reported in Figure 10, it is difficult to correlate the extent of DNA release (Figure 9) with the size and ζ-potential of complexes emerging from interaction with cellular lipids. Electrophoresis results (Figure 9) show that for $R < 0.5$ DNA is almost completely released from LPD systems, while it is still largely protected by lipoplexes. As a whole, these results indicate that the size and ζ-potential of complexes interacting with cellular lipids are mainly regulated by the anionic/cationic charge ratio, *R*, while the ability of the investigated formulations to release DNA is controlled by factors other than *R*. The DNA release ability may be connected with the membrane fusion rate of complexes with cellular membranes that is, in turn, inversely related to the multilamellarity of lipid aggregates. Such suggestion is in good agreement with SAXS findings (Figure 7) showing that lipoplexes are multilamellar systems, while LPD nanoparticles are made of a few membranes and are therefore more disposed to fuse with ALs mimicking cellular membranes and to release their gene cargo.

Cell Imaging. Confocal images of CHO-K1 cells 4 h after incubation with LPD complexes and DOTAP/DNA lipoplexes ($R_V = 2$) are shown in Figure 11. We observe that green fluorescence from lipids forming LPD nanoparticles was clearly localized, while DNA (red fluorescence) had visibly spread into the cytoplasm (Figure11A). It may be reasonable to judge such spreading red regions as due to plasmid DNA exiting from the endosomal or lysosomal stage into the cytoplasm. Over the same time scale, CHO-K1 cells incubated with DOTAP/DNA lipoplexes were mainly distributed throughout the cytoplasm and to some extent at the cell periphery (Figure 11B). Complexes appeared almost devoid of cytoplasmic plasmid DNA, suggesting that such binary formulation is defective in facilitating endosomal escape of nucleic acids, resulting in entrapment of plasmid DNA in endosomes. Since there is a possibility that lipoplexes exhibit DNA release with different kinetics than LPD complexes, the distribution was followed at various time points (4, 6, 8, 10, 12, 24, 36, and 48 h). Over such time scale, significant cytosolic DNA release from lipoplexes as that observed for LPD nanoparticles was not detected.

■ DISCUSSION

This study represents a direct comparison between a pDNA-encapsulated system (LPD) and a complex system (lipoplex) on

dx.doi.org/10.1021/jm200237p |*J. Med. Chem.* 2011, 54, 4160–4171

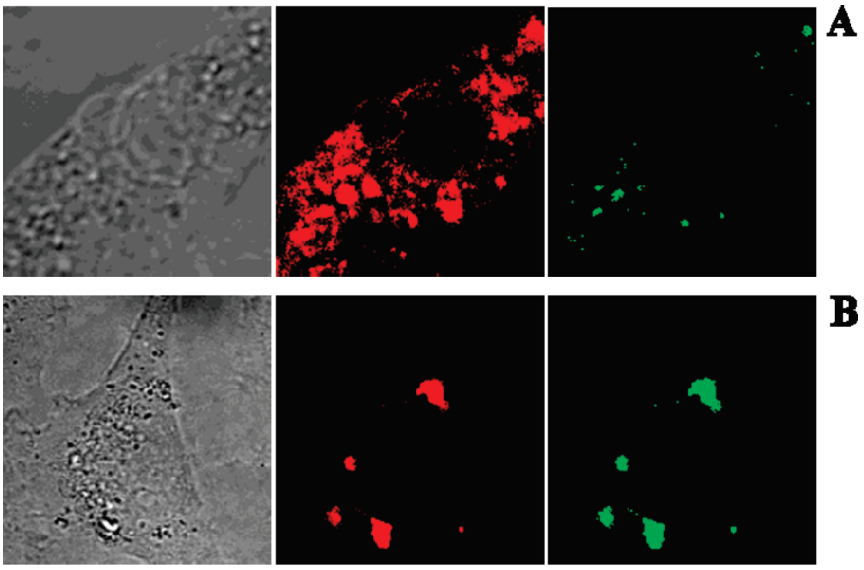

Figure 11. Confocal microscopy of CHO-K1 cells 4 h after treatment with LPD complexes (A) and lipoplexes (B). Green fluorescence from NBD lipids forming LPD complexes was clearly localized, while DNA (red fluorescence) had visibly spread into the cytoplasm. DOTAP/DNA lipoplexes were distributed throughout the cytoplasm and to some extent at the cell periphery. Colocalization of green and red fluorescence signals suggests that lipoplexes are intact with DNA trapped within.

the basis of the same lipid composition. Crucial to the mechanism of gene delivery is likely the relative ease by which the gene and amphiphile dissociate. Insight into parameters that determine stabilization and destabilization of these complexes, which are intricately related to their efficiency in gene delivery, requires an understanding of factors that govern amphiphile−DNA interaction and subsequent complex formation. Upon complex formation, reentrant condensation and charge inversion[20,21] occurred in both systems (Figure 3). Both charge inversion and charge and size saturation of LPD complexes were found to occur at R_V values smaller than those observed when lipoplexes were used. This finding means that complete encapsulation of protamine/DNA core by a lipid envelope requires a lower amount of cationic lipid than that needed to condense the same amount of DNA by a lipoplex system. Toxicity of the complex, as described for many such complexes, may depend upon the amount of cationic lipid used to transfect cells. Pertinent to sustaining such toxicity effects may be their biodegradability and the cell's capacity to eliminate cationic lipids. Thus, LPD complexes, because of the lower amount of cationic lipid needed to protect DNA, are potentially less toxic than lipoplexes.

We found that TE of LPD nanoparticles was higher than that of lipoplexes in all the tested cell lines (Figure 8). DNA complexes must overcome a series of barriers to gain access to the membrane surface, cytoplasmic compartment, and nucleus of a target cell and to translate transgenes into protein. As particles encounter each of these barriers, they are subject to a certain probability of success or failure in overcoming each. The cumulative probability of success for the entire journey is reflected in the transfection efficiency for a given system.[39] A number of physical−chemical properties of lipoplexes have been proposed as factors regulating success in overcoming such transfection barriers such as size,[40−43] ζ-potential,[44,45] nanostructure,[22,46] propensity to be disintegrated by anionic lipids,[20,21,35−38,47] and ability to release DNA both in the cytosol and in the nucleus.

Upon arrival near the cell, complexes associate electrostatically with mammalian cells, which contain surface proteoglycans with negatively charged sulphated groups. Since the first interaction between nanocarriers and cells is charge-mediated and not specific, complexes with high ζ-potential are supposed to be better internalized. A preferential binding should result in subsequent efficient cellular internalization of the carrier−DNA complex that is crucial to nonviral gene transfer. However, ζ-potential of LPD complexes and lipoplexes were found to be roughly the same (ζ_p = 47.5 and 44.4 mV, respectively). Thus, charge-mediated efficient binding played a minor role, if any, in differentiating efficiency levels of the two carriers.

Nonviral vectors can be transported to the cytoplasmic compartment by a diversity of endocytic mechanisms.[39] Each of these pathways may support a different level of transfection mediated by a given delivery system. An emerging paradigm for the design of effective gene carriers is the modification of particulate parameters to encourage entry via a preferable endocytic pathway.[48,49] The endocytic machinery and cell membrane have well-defined geometries and flexibility that may restrict entry of incompatibly large or small particles.[40−43] Recently, a size-dependent mechanism of lipoplex internalization has been proposed.[41] Accordingly, complexes with a size of approximately 200 nm or less are supposed to enter cells basically via the clathrin-coated pathway, while larger complexes are internalized via caveolae-mediated pathways. Our DLS data show that both LPD complexes and lipoplexes used in the present study are larger than 200 nm in size. Even though a precise determination of the internalization mechanisms of LPD complexes and lipoplexes is beyond the scope of the present study, we claim that potential differences in their internalization efficiency, if any, should not be size regulated. In summary, size and surface charge of complexes could not be taken into account to justify differences in TE.

It is the surface of the gene delivery system that is recognized and processed by cells, and this has important implications for safety considerations and the practice of nanomedicine.[30−33] From this point of view, surface properties of LPD complexes and lipoplexes were found to be largely different from each other.

Proteomics experiments (Figure 5, top) showed that surface of LPD complexes resembles that of pure DOTAP CLs while that of lipoplexes is partly decorated with adsorbed DNA molecules. The latter finding is in very good agreement with the recent suggestion that the position of the negatively charged DNA is not controlled in the lipoplex system.[19] This aspect is potentially detrimental for in vivo application because interactions between negatively charged DNA and positively charged serum components have been found to result in the formation of large aggregates and would also result in undesirable lung accumulation. On the other side, encapsulating pDNA in the lipid envelope would be an ideal strategy to shield the mutual interactions between DNA and basic serum proteins.[10,12−18]

When in the cytosol, the ability of a nonviral vector to escape from the endosomal compartment determines the carrier's transfection ability. Exposure to the acidic and degradative lysosomal compartment reduces the transfection efficiency of nonviral vectors. Therefore, enhanced escape from the acidic endosomes by the proton sponge effect[50] or by chemical and physical endosomolytic agents[51] has been pursued to help surmount this cytoplasmic barrier. Most lipid/DNA complexes are ordered structures. In cells, they may be presumed to interact with a number of cellular membranes, during which DNA may be released gradually only after the lipoplex has acquired enough anionic lipids to neutralize the cationic charge and to rearrange into a structure from which the DNA can escape. Thus, intermixing of cellular lipids with lipoplex lipids is presumed to be a necessary step in transfection.[52] Upon nanocarrier−cellular membrane interaction, anionic cellular lipids laterally diffuse into the complex and locally neutralize cationic lipids.[52] Formation of cationic/anionic mixed bilayers is expected to weaken the electrostatic attraction between cationic lipoplex lipids and anionic DNA molecules. Only when the membrane charge density of cationic membranes is completely neutralized by anionic lipids does DNA start to escape from complexes appreciably.[53] SAXS measurements showed that DNA is not present in the lipid envelope of LPD complexes, but it is confined in the central core. Thus, anionic cellular lipids can interact with cationic lipids of LPD complexes without competing with DNA molecules. According to electrostatic interaction models,[52,53] we hypothesize that the absence of electrostatic competition between ALs and DNA molecules would result in the high incorporation efficiency of ALs within LPD membranes, resulting in the efficient DNA cytoplasmic release observed by confocal microscopy experiments (Figure 11). Numerous contacts visualized by electron microscopy between lipoplexes and various cellular membranes[54] support a concept of gradual lipoplex peeling and DNA release. SAXS measurements reported in Figure 7 show that LPD complexes are made of about 10 lipid layers in a highly swollen state, while lipoplexes are well ordered multilamellar structures made of more than 30 alternating lipid/DNA layers. Given the need for intermixing of anionic cellular lipids and cationic carrier lipids,[52−58] our findings take on a particular significance because the ability of ALs to initiate DNA release could depend on the extent of membrane fusion (strictly, lipid mixing) between anionic cellular membranes and lipid carriers. All these suggestions are well supported by results reported in Figure 9 showing a plain correlation between complexes and their ability to release DNA upon interaction with cellular lipids.

Figure 12 summarizes our present understanding of mechanisms occurring upon complex−cell interaction. Because of similar size and ζ-potential, as well as identical lipid composition, it is reasonable that complexes enter the cell using similar internalization mechanisms. However, after complex internalization within cells, both LPD complexes and lipoplexes must fuse with the negatively charged cellular membrane to escape endosomes. LPD complexes are more fusogenic than lipoplexes, a phenomenon that is presumably related to higher interaction between cationic and anionic cellular lipids due to the absence of competing DNA in the lipid envelope and to the lower number of lipid layers to be peeled off. If poor DNA release from lipoplexes proves to be a critical attribute of poor transfection, an intelligent strategy to achieve efficient dissociation of pDNA is desirable. Collectively, these data support the hypothesis that the encapsulation of pDNA in the lipid envelope has a distinct advantage for releasing DNA in the cytosol. As for intranuclear disposition of the DNA cargo, coating the core with the minimum number of fusogenic lipid envelopes ensuring complete DNA protection is ideal for decoating and for facilitated release.

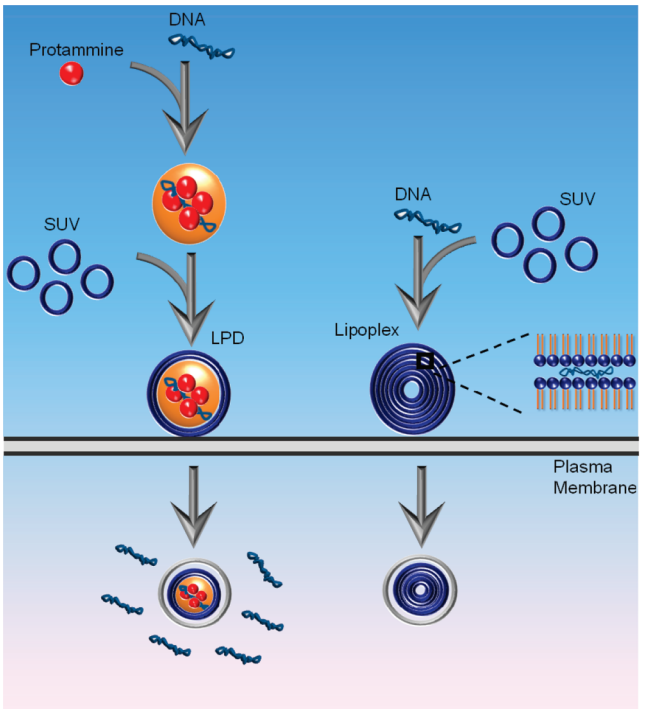

Figure 12. Because of comparable size and ζ-potential, as well as identical lipid composition, it is reasonable to judge that LPD complexes and lipoplexes enter the cell using similar internalization mechanisms. However, after complex internalization, both LPD complexes and lipoplexes fuse with the negatively charged endosomal membrane. LPD complexes are more fusogenic than lipoplexes, a phenomenon that is presumably related to higher interaction between cationic and anionic cellular lipids due to the absence of competing DNA in the lipid envelope and to the lower number of lipid layers to be peeled off. DNA release from endosomes is not a relevant barrier for LPD complexes, while DOTAP/DNA lipoplexes remained largely intact and accumulated at the nuclear membrane without releasing DNA abundantly.

CONCLUSIONS

The findings reported herein indicate that a LPD system is more efficient in transfecting cells if compared to the consolidated lipoplex strategy. Such a system has evident advantage in terms of endosomal escape and DNA release. Encapsulating

pDNA in the lipid envelope would also be an ideal strategy to shield the mutual interactions between DNA and basic serum proteins for in vivo applications as well as to better investigate the interaction between nanocarriers and cellular compartments. The findings reported in this study promise to be useful for the development of efficient gene delivery systems for both in vitro and in vivo applications. In the near future, the very same packaging strategy will be applied to develop a proper LPD system equipped with functional devices to control intracellular fate and intranuclear DNA release. This functionalized envelope-type system will be able to compete with the efficiency of viral vectors.

EXPERIMENTAL SECTION

Liposomes. Cationic 1,2-dioleoyl-3-trimethylammonium propane (DOTAP) and fluorescently labeled NBD-DOTAP were purchased from Avanti Polar Lipids (Alabaster, AL) and used without further purification. DOTAP cationic liposomes (CLs) were prepared according to standard protocols.[59] In brief, the proper amount of DOTAP was dissolved in chloroform and the solvent was evaporated under vacuum for at least 24 h. The obtained lipid films were hydrated with the appropriate amount of Tris-HCl buffer solution (10^{-2} M, pH 7.4) to achieve the desired final concentration (1 mg/mL). The same experimental protocol was used to prepare negatively charged liposomes made of anionic lipids dioleoylphosphatidylglycerol (DOPG) and dioleoylphosphatidic acid (DOPA). Liposome dispersions were sonicated to clarity to prepare SUVs.

LPD Complexes. Protamine sulfate salt (P) from salmon (MW = 5.1 kDa) was purchased from Sigma-Aldrich (St. Louis, MO). For dynamic light scattering, synchrotron small-angle X-ray scattering (SAXS), and electrophoresis experiments, calf thymus DNA was used. For confocal fluorescence microscopy experiments, Cy3-labeled 2.7 kbp plasmid DNA (Mirus Bio Corporation, Madison, WI) was used. Positively charged P/DNA microspheres were prepared at seven protamine/DNA weight ratios R_W = 0.25, 0.5, 1, 2, 3, 5, and 10. Positively charged P/DNA microspheres at R_W = 0.5 were mixed with DOTAP SUVs at nine lipid/DNA volume ratios, R_V = 0.25, 0.5, 1, 1.25, 1.75, 2, 3, 5, and 10.

Lipoplexes. When adequate amounts of the DNA solutions were mixed with suitable volumes of DOTAP liposome dispersions, self-assembled DOTAP/DNA lipoplexes at nine volume ratios R_V = 0.25, 0.5, 1, 1.25, 1.75, 2, 3, 5, and 10 were obtained.

Size and ζ-Potential. The size and size distribution of CLs, LPD, and lipoplexes were measured at 25 °C by a Malvern NanoZetaSizer spectrometer equipped with a 5 mW HeNe laser (wavelength λ = 632.8 nm) and a digital logarithmic correlator. The normalized intensity autocorrelation functions were detected at 90° and analyzed by using the CONTIN method, which analyzes the autocorrelation function through an inverse Laplace transform[60,61] in order to obtain the distribution of the diffusion coefficient D of the particles. This coefficient is converted into an effective hydrodynamic radius R_H by using the Stokes−Einstein relationship $R_H = K_BT/(6\pi\eta D)$, where K_BT is the thermal energy and η the solvent viscosity. Our clusters invariably show a size distribution, and the values of the radii reported here correspond to the so-called "intensity weighted" average.[62] The electrophoretic mobility measurements were carried out by means of the laser Doppler electrophoresis technique, the same apparatus used for size measurements. The mobility u was converted into the ζ-potential using the Smoluchowski relation $\zeta = u\eta/\varepsilon$, where η and ε are the viscosity and the permittivity of the solvent phase, respectively.

One-Dimensional Polyacrylamide Gel Electrophoresis (1D-PAGE). Human plasma was prepared as described elsewhere.[63] An amount of 100 μL of CL, LPD, and lipoplex suspensions (1 mg/mL) were incubated with 100 μL of plasma on ice. The samples were centrifuged to pellet the particle−protein complexes. The pellet was resuspended in phosphate buffered saline (PBS), transferred into a new vial, and centrifuged again to pellet the particle−protein complexes; this procedure was repeated twice. The proteins were eluted from the particles by adding sodium dodecyl sulfate (SDS) sample buffer to the pellet and boiling the solution. Then the proteins were separated by 10% 1D SDS−PAGE gels. Coomassie PhastGel Blue R-350 was used to stain the gels with gentle agitation, in accordance with the manufacturer's manual (GE Healthcare, Milan, Italy). All experiments were conducted four times to ensure reproducibility of the particle−protein complex pellet sizes, general pattern, and band intensities on the 1D gels. To determine molecular weights of proteins after electrophoretic run, protein molecular weight markers were used. The molecular weights were finally obtained by means of the dedicated software Kodak (Rochester, NY).

Synchrotron Small Angle X-ray Scattering. SAXS measurements were performed at the Austrian SAXS station of the synchrotron light source ELETTRA (Trieste, Italy).[64] SAXS patterns were recorded with gas detectors based on the delay line principle covering the q-ranges from q_{min} = 0.04 $Å^{-1}$ to q_{max} = 0.5 $Å^{-1}$ with a resolution of 5×10^{-4} $Å^{-1}$ (fwhm). The angular calibration of the detectors was performed with silver behenate powder (d-spacing of 58.38 Å). The data have been normalized for variations of the primary beam intensity, corrected for the detector efficiency, and the background has been subtracted. Exposure times were typically 300 s. No evidence of radiation damage was observed in the X-ray diffraction patterns. In both experimental sessions the sample was held in a 1 mm glass capillary (Hilgenberg, Malsfeld, Germany) and the measurements were performed at 25 °C with a precision of 0.1 °C.

Transfection Efficiency. Transfection efficiency is evaluated by the expression of reporter firefly luciferase gene and measured by the luciferase reporter assay. Fibroblasts 3T3 NIH, CHO, Hek293, and A17[65] cells were cultured in Dulbecco's modified Eagle's medium (DMEM) with GlutaMAX-I (Invitrogen) supplemented with 10% fetal bovine serum (FBS, Invitrogen) at 37 °C and 5% CO_2 atmosphere, splitting cells every 2−4 days to maintain monolayer coverage. Twenty-four hours before transfection 150 000 cells were seeded per well into 24-well culture plates in order to reach 70−80% confluence during transfection. For transfection experiments, plasmid DNA (pGL3 control vector, which codifies for firefly luciferase under the control of SV40 promoter) (Promega, Madison, WI) was employed. Both LPD nanoparticles and lipoplexes were prepared at a fixed lipid/DNA volume ratio, R_V = 2. This value was chosen because it corresponds to a typical plateau value. LPD complexes and lipoplexes were prepared in Optimem (Invitrogen) by mixing, for each well of 24-well plates, 0.5 μg of pDNA, condensed or not with protamine, with 10 μL of sonicated lipid dispersion (0.5 mg/mL). These complexes were left for 20 min at room temperature before adding them to the cells. The cells were incubated with lipoplexes in Optimem (Invitrogen) for 3 h to permit transient transfection before they were incubated in 1 mL of growth medium for 24 h. Finally, cells were whashed in PBS and harvested in 200 μL of 1× reporter lysis buffer (Promega). Of the cell suspension 20 μL was diluted in 100 μL of luciferase reaction buffer (Promega), and the luminescence was measured after 10 s using a luminometer (Berthold). Results were espressed as relative light units per mg of cell proteins as determined by Bio-Rad protein assay dye reagent (Bio-Rad). Each condition was performed in quadruplicate and repeated three times.

Electrophoresis on Agarose Gels. Electrophoresis studies were conducted on 1% agarose gel containing ethidium bromide in Tris−borate−EDTA (TBE) buffer as elsewhere described.[58] LPD complexes and lipoplexes were prepared by mixing 4 μg of pDNA, condensed or not with protamine, with 45 μL of lipid dispersion (1 mg/mL DOTAP). These complexes were left for 20 min at room temperature before

incubating them with (i) Tris-HCl buffer solution (incubation time 0−3 h), (ii) fetal bovine serum (FBS) (incubation time 0−3 h), and negatively charged liposomes (DOPA, DOPG) (incubation time 1 h). Naked plasmid DNA, P/DNA microspheres, LPD complexes, and lipoplexes (upon interaction with Tris-HCl buffer solution, serum, and cellular lipids at different *R* values) were analyzed by electrophoresis. For this purpose, 10 μL of each sample was mixed with 2 μL of loading buffer (glycerol 30%, bromophenol blue 0.25%) and subjected to agarose gel electrophoresis for 1 h at 80 V. The electrophoresis gel was visualized and digitally photographed using a Kodak image station, model 2000 R (Kodak, Rochester, NY). Digital photographs were enhanced using dedicated software (Kodak MI, Kodak).[66]

Confocal Fluorescence Microscopy Experiments. Chinese hamster ovary (CHO-K1) cells were cultured and maintained in a humidified, 5% CO_2 atmosphere at 37 °C in Dulbecco's modified Eagle's medium (Gibco, Paisley, U.K.) supplemented with 10% fetal bovine serum and nonessential amino acids, splitting the cells every 2−4 days to maintain monolayer coverage. For transfection experiments, lipoplexes were prepared in PBS (Invitrogen, Carlsbad, CA) by mixing 0.5 μg of Cy3-labeled plasmid DNA with 10 μL of sonicated lipid dispersions. These complexes were left for 20 min at room temperature before adding them to the cells. Confocal fluorescence microscopy experiments were performed with the Olympus Fluoview 1000 (Olympus, Melville, NY) confocal microscope.

■ ASSOCIATED CONTENT

Supporting Information. DNA condensation by lipoplexes and LPD nanoparticles from UV−vis absorption measurements; size and ζ potential of complexes followed in time over 24 h. This material is available free of charge via the Internet at http://pubs.acs.org.

■ AUTHOR INFORMATION

Corresponding Author
*Phone: 39 06 49693271. Fax: 39 06 490631. E-mail: giulio.caracciolo@uniroma1.it.

■ ACKNOWLEDGMENT

This work was partially supported by the Italian Minister for University and Research (MIUR) (Futuro in Ricerca, Grant No. RBFR08TLPO).

■ ABBREVIATIONS USED

LDP, lipid/DNA/polycation; TE, transfection efficiency; CL, cationic liposome; SDS−PAGE, sodium dodecyl sulfate−polyacrylamide gel electrophoresis; AL, anionic lipid

■ REFERENCES

(1) Felgner, P. L.; Ringold, G. M. Cationic liposome-mediated transfection. *Nature* **1989**, *337*, 387–388.
(2) Marshall, E. Gene therapy: what to do when clear success comes with an unclear risk?. *Science* **2002**, *288*, 951–952.
(3) Ramezani, M.; Khoshhamdam, M.; Dehshari, A.; Malaekeh-Nikouei, B. The influence of size, lipid composition and bilayer fluidity of cationic liposomes on the transfection efficiency of nanolipoplexes. *Colloids Surf., B* **2009**, *72*, 1–5.
(4) Raëdler, J. O.; Koltover, I.; Salditt, T.; Safinya, C. R. Structure of DNA−cationic liposome complexes: DNA intercalation in multilamellar membranes in distinct interhelical packing regimes. *Science* **1997**, *275*, 810–814.
(5) Salditt, T.; Koltover, I.; Raëdler, J. O.; Safinya, C. R. Two-dimensional smectic ordering of linear DNA chains in self-assembled DNA−cationic liposome mixtures. *Phys. Rev. Lett.* **1997**, *79*, 2582–2585.
(6) Artzner, F.; Zantl, R.; Rapp, G.; Raëdler, J. O. Observation of a rectangular columnar phase in condensed lamellar cationic lipid−DNA complexes. *Phys. Rev. Lett.* **1998**, *81*, 5015–5018.
(7) Caracciolo, G.; Caminiti, R.; Natali, F.; Castellano, A. C. A new approach for the study of cationic lipid−DNA complexes by energy dispersive X-ray diffraction. *Chem. Phys. Lett.* **2002**, *366*, 200–204.
(8) Sternberg, B.; Sorgi, F. L.; Huang, L. New structures in complex formation between DNA and cationic liposomes visualized by freeze−fracture electron microscopy. *FEBS Lett.* **1994**, *356*, 361–366.
(9) Mönkkönen, J.; Urtti, A. Lipid fusion in oligonucleotide and gene delivery with cationic lipids. *Adv. Drug Delivery Rev.* **1998**, *34*, 37–49.
(10) Zuhorn, I. S.; Visser, W. H.; Bakowsky, U.; Engberts, J. B; Hoekstra, D. Interference of serum with lipoplex−cell interaction: modulation of intracellular processing. *Biochim. Biophys. Acta* **2002**, *1560*, 25–36.
(11) Elouahabi, A.; Ruysschaert, J. M. Formation and intracellular trafficking of lipoplexes and poliplexes. *Mol. Ther.* **2005**, *11*, 336–347.
(12) Kogure, K.; Moriguchi, R.; Sasaki, K.; Ueno, M.; Futaki, S.; Harashima, H. Development of efficient packaging method of oligodeoxynucleotides by a condensed nano particle in lipid envelope structure. *J. Controlled Release* **2004**, *98*, 317–323.
(13) Yamauchi, J.; Hayashi, Y.; Kajimoto, K.; Akita, H.; Harashima, H. Comparison between a multifunctional envelope-type nano device and lipoplex for delivery to the liver. *Biol. Pharm. Bull.* **2010**, *33*, 926–929.
(14) Tan, Y.; Whitmore, M.; Li, S.; Frederik, P.; Huang, L. LPD nanoparticles—novel nonviral vector for efficient gene delivery. *Methods Mol. Med.* **2002**, *69*, 73–81.
(15) Li, S. D.; Huang, L. Surface-modified LPD nanoparticles for tumor targeting. *Ann. N.Y. Acad. Sci.* **2006**, *1082*, 1–8.
(16) Chen, Y.; Sen, J.; Bathula, S. R.; Yang, Q.; Fittipaldi, R.; Huang, L. Novel cationic lipid that delivers siRNA and enhances therapeutic effect in lung cancer cells. *Mol. Pharmaceutics* **2009**, *6*, 696–705.
(17) Chen, Y.; Bathula, S. R; Li, J.; Huang, L. Multifunctional nanoparticles delivering small interfering RNA and doxorubicin overcome drug resistance in cancer. *J. Biol. Chem.* **2010**, *285*, 22639–22650.
(18) Yang, X.; Peng, Y.; Yu, B.; Yu, J.; Zhou, C.; Mao, Y.; Lee, L. J.; Lee, R. J. A covalently stabilized lipid−polycation−DNA (sLPD) vector for antisense oligonucleotide delivery. *Mol Pharmaceutics* [Online early access]. DOI: 10.1021/mp100272k. Published Online: Mar 2, **2011**.
(19) Amenitsch, H.; Caracciolo, G.; Foglia, P.; Fuscoletti, V.; Giansanti, P; Marianecci, C.; Pozzi, D.; Laganà, A. Existence of hybrid structures in cationic liposome/DNA complexes revealed by their interaction with plasma proteins. *Colloid Surf., B* **2011**, *82*, 141–146.
(20) Caracciolo, G.; Pozzi, D.; Caminiti, R.; Marchini, C.; Montani, M.; Amici, A.; Amenitsch, A. On the correlation between phase evolution of lipoplexes/anionic lipid mixtures and DNA release. *Appl. Phys. Lett.* **2007**, *91*, 143903.
(21) Caracciolo, G.; Marchini, C.; Pozzi, D.; Caminiti, R.; Amenitsch, H.; Montani, M.; Amici, A. Structural stability against disintegration by anionic lipids rationalizes the efficency of cationic liposom/DNA complexes. *Langmuir* **2007**, *23*, 4498–4508.
(22) Pozzi, D.; Caracciolo, G.; Caminiti, R.; Candeloro De Sanctis, S.; Amenitsch, H.; Marchini, C.; Montani, M.; Amici, A. Toward the rational design of lipid gene vectors: shape coupling between lipoplex and anionic cellular lipids controls the phase evolution of lipoplexes and the efficiency of DNA release. *ACS Appl. Mater. Interfaces* **2009**, *10*, 2237–2249.
(23) Caracciolo, G.; Pozzi, D.; Amici, A.; Amenitsch, H. Universality of DNA adsorption behavior on the cationic membranes of nanolipoplexes. *J. Phys. Chem. B* **2010**, *114*, 2028–2032.
(24) Caracciolo, G.; Caminiti, R. DNA−DNA electrostatic interactions within cationic lid/DNA lamellar complexes. *Chem. Phys. Lett.* **2004**, *400*, 314–319.

(25) Zuzzi, S.; Cametti, C.; Onori, G. Polyion-induced aggregation of lipidic-coated solid polystyrene spheres: the many facets of complex formation in low-density colloidal suspensions. *Langmuir* **2008**, *24*, 6044–6049.

(26) Zuzzi, S.; Cametti, C.; Onori, G.; Sennato, S.; Tacchi, S. Polyion-induced cluster formation in different colloidal polyparticle aqueous suspensions. *Langmuir* **2009**, *25*, 5910–5917.

(27) Dunne, M.; Bibby, D. C.; Jones, J. C.; Cudmore, S. Encapsulation of protamine sulphate compacted DNA in polylactide and polylactide-*co*-glycolide microparticles. *J. Controlled Release* **2003**, *92*, 209–219.

(28) Marty, R.; N'soukpoé-Kossi, C. N.; Charbonneau, D.; Weinert, C. M.; Kreplak, L.; Tajmir-Riah, H.-A. Structural analysis of DNA complexation with cationic lipids. *Nucleic Acids Res.* **2009**, *37*, 849–857.

(29) Chesnoy, S.; Huang, L. Structure and function of lipid-DNA complexes for gene delivery. *Annu. Rev. Biophys. Biomol. Struct.* **2000**, *29*, 27–47.

(30) Cedervall, T.; Lynch, I.; Lindman, S.; Berggård, T.; Thulin, E.; Nilsson, H.; Dawson, K. A.; Linse, S. Understanding the nanoparticle–protein corona using methods to quantify exchange rates and affinities of proteins for nanoparticles. *Proc. Natl. Acad. Sci. U.S.A.* **2007**, *104*, 2050–2055.

(31) Lundqvist, M.; Stigler, J.; Elia, G.; Lynch, I.; Cedervall, T.; Dawson, K. A. Nanoparticle size and surface properties determine the protein corona with possible implications for biological impacts. *Proc. Natl. Acad. Sci. U.S.A.* **2008**, *105*, 14265–14270.

(32) Monopoli, M. P.; Walczyk, D.; Campbell, A.; Elia, G.; Lynch, I.; Baldelli Bombelli, F.; Dawson, K. A. Physical–chemical aspects of protein corona: relevance to in vitro and in vivo biological impacts of nanoparticles. *J. Am. Chem. Soc.* **2010**, *133*, 2525–2534.

(33) Caracciolo, G.; Callipo, L.; Candeloro De Sanctis, S.; Cavaliere, C.; Pozzi, D.; Laganà, A. Surface adsorption of protein corona controls the cell internalization mechanism of DC-Chol–DOPE/DNA lipoplexes in serum. *Biochim. Biophys. Acta* **2010**, *1798*, 536–543.

(34) Deng, Z. J.; Mortimer, G.; Schiller, T.; Musumeci, A.; Martin, D.; Minchin, R. F. Differential plasma protein binding to metal oxide nanoparticles. *Nanotechnology* **2009**, *20*, 455101.

(35) Yury, S.; Tarahovsky, Y.; Koynova, R.; MacDonald, R. C. DNA release from lipoplexes by anionic lipids: correlation with lipid mesomorphism, interfacial curvature, and membrane fusion. *Biophys. J.* **2004**, *87*, 1054–1064.

(36) Koynova, R.; Wang, L.; Tarahovsky, Y.; MacDonald, R. C. Lipid phase control of DNA delivery. *Bioconjugate Chem.* **2005**, *16*, 1335–1339.

(37) Koynova, R.; MacDonald, R. C. Lipid transfer between cationic vesicles and lipid–DNA lipoplexes: effect of serum. *Biochim. Biophys. Acta* **2005**, *1714*, 63–70.

(38) Koynova, R.; Wang, L.; MacDonald, R. C. An intracellular lamellar–nonlamellar phase transition rationalizes the superior performance of some cationic lipid transfection agents. *Proc. Natl. Acad. Sci. U.S.A.* **2006**, *103*, 14373–14378.

(39) Adler, A. F.; Leong, K. W. Emerging links between surface nanotechnology and endocytosis: impact on nonviral gene delivery. *Nano Today* **2010**, *5*, 553–569.

(40) Almofti, M. R.; Harashima, H.; Shinohara, Y.; Almofti, A.; Li, W. H.; Kiwada, H. Lipoplex size determines lipofection efficiency with or without serum. *Mol. Membr. Biol.* **2003**, *20*, 35–43.

(41) Rejman, J.; Oberle, V.; Zuhorn, I. S.; Hoekstra, D. Size-dependent internalization of particles via the pathways of clathrin- and caveole-mediated endocytosis. *Biochem. J.* **2004**, *377*, 159–169.

(42) Rejman, J.; Conese, M.; Hoekstra, D. Gene transfer by means of lipo- and polyplexes: role of clathrin and caveole-mediated endocytosis. *J. Liposome Res.* **2006**, *16*, 237–247.

(43) Hoekstra, D.; Rejman, J.; Wasungu, L.; Shi, F.; Zuhorn, I. Gene delivery by cationic lipids: in and out of an endosome. *Biochem. Soc. Trans.* **2007**, *35*, 68–71.

(44) Yang, J. P.; Huang, L. Overcoming the inhibitory effect of serum on lipofection by increasing the charge ratio of cationic liposome to DNA. *Gene Ther.* **1997**, *4*, 950–960.

(45) Zelphati, O.; Uyechi, L. S.; Barron, L. G.; Szoka, F. C., Jr. Effect of serum components on the physico-chemical properties of cationic lipid/oligonucleotide complexes and on their interactions with cells. *Biochim. Biophys. Acta* **1998**, *1390*, 119–133.

(46) Caracciolo, G.; Pozzi, D.; Caminiti, R.; Congiu Castellano, A. Structural characterization of a new lipid/DNA complex showing a selective transfection efficiency in ovarian cancer cells. *Eur. Phys. J. E* **2003**, *10*, 331–336.

(47) Caracciolo, G.; Pozzi, D.; Caminiti, R.; Marchini, C.; Montani, M.; Amici, A.; Amenitsch, H. Transfection efficiency boost by designer multicomponent lipoplexes. *Biochim. Biophys. Acta* **2007**, *1768*, 2280–2292.

(48) Akita, H.; Kudo, A.; Minoura, A.; Yamaguti, M.; Khalil, I. A.; Moriguchi, R.; Masuda, T.; Danev, R.; Nagayama, K.; Kogure, K.; Harashima, H. Multi-layered nanoparticles for penetrating the endosome and nuclear membrane via a step-wise membrane fusion process. *Biomaterials* **2009**, *30*, 2940–2949.

(49) Akita, H.; Kogure, K.; Moriguchi, R.; Nakamura, Y.; Higashi, T.; Nakamura, T.; Serada, S.; Fujimoto, M.; Naka, T.; Futaki, S.; Harashima, H. Nanoparticles for ex vivo siRNA delivery to dendritic cells for cancer vaccines: programmed endosomal escape and dissociation. *J. Controlled Release* **2010**, *143*, 311–317.

(50) Sonawane, N. D.; Szoka, F. C., Jr.; Verkman, A. S. Chloride accumulation and swelling in endosomes enhances DNA transfer by polyamine–DNA polyplexes. *J. Biol. Chem.* **2003**, *278*, 44826–44831.

(51) Wagner, E. Effects of membrane-active agents in gene delivery. *J. Controlled Release* **1998**, *53*, 155–158.

(52) Xu, Y. H.; Szoka, F. C. Mechanism of DNA release from cationic liposome/DNA complexes used in cell transfection. *Biochemistry* **1996**, *35*, 5616–5623.

(53) Caracciolo, G.; Pozzi, D.; Amenitsch, H.; Caminiti, R. Interaction of lipoplexes with anionic lipids resulting in DNA release is a two-stage process. *Langmuir* **2007**, *23*, 8713–8717.

(54) Koynova, R.; Tarahovsky, Y.; Wang, L.; MacDonald, R. C. Lipoplex formulation of superior efficacy exhibits high surface activity and fusogenicity, and readily releases DNA. *Biochim. Biophys. Acta* **2007**, *1768*, 375–386.

(55) Kozlov, M. M.; Markin, V. S. On the theory of membrane fusion. The adhesion–condensation mechanism. *Gen. Physiol. Biophys.* **1984**, *5*, 379–402.

(56) Pantazatos, D. P.; Pantazatos, S. P.; MacDonald, R. C. Bilayer mixing, fusion, and lysis following the interaction of populations of cationic and anionic phospholipid bilayer vesicles. *J. Membr. Biol.* **2003**, *194*, 129–139.

(57) Hed, G.; Safran, S. A. Attractive instability of oppositely charged membranes induced by charge density fluctuations. *Phys. Rev. Lett.* **2004**, *93*, 138101.

(58) Marchini, C.; Pozzi, D.; Montani, M.; Alfonsi, C.; Amici, A.; Amenitsch, H.; Candeloro De Sanctis, S.; Caracciolo, G. Tailoring lipoplex composition to the lipid composition of plasma membrane: a Trojan horse for cell entry?. *Langmuir* **2010**, *26*, 13867–13873.

(59) Caracciolo, G.; Pozzi, D.; Caminiti, R. Lipid mixing upon deoxyribonucleic acid-induced liposomes fusion investigated by synchrotron small-angle X-ray scattering. *Appl. Phys. Lett.* **2005**, *87*, 133901.

(60) Provencher, S. W. A constrained regularization method for inverting data represented by linear algebraic or integral equations. *Comput. Phys. Commun.* **1982**, *27*, 213–227.

(61) Provencher, S. W. CONTIN: a general purpose constrained regularization program for inverting noisy linear algebraic and integral equations. *Comput. Phys. Commun.* **1982**, *27*, 229–242.

(62) Berne, B. J.; Pecora, R. *Dynamic Light Scattering: With Applications to Chemistry, Biology, and Physics*; Dover Publications Inc.: New York, 2003.

(63) Caracciolo, G.; Callipo, L.; Candeloro De Sanctis, S.; Cavaliere, C.; Pozzi, D.; Laganà, A. Surface adsorption of protein corona controls the cell internalization mechanism of DC-Chol–DOPE/DNA lipoplexes in serum. *Biochim. Biophys. Acta* **2010**, *1798*, 536–543.

(64) Amenitsch, H.; Rappolt, M.; Kriechbaum, M.; Mio, H.; Laggner, P.; Bernstorff, S. First performance assessment of the small-angle X-ray scattering beamline at ELETTRA. *J. Synchrotron Radiat.* **1998**, *5*, 506–508.

(65) Galiè, M.; D'Onofrio, M.; Montani, M.; Amici, A.; Calderan, L.; Marzola, P.; Benati, D.; Merigo, F.; Marchini, C.; Sbarbati, A. Tumor vessel compression hinders perfusion of ultrasonographic contrast agents. *Neoplasia* **2005**, *7*, 528–536.

(66) Caracciolo, G.; Pozzi, D.; Caminiti, R.; Marchini, C.; Montani, M.; Amici, A.; Amenitsch, H. DNA release from cationic liposome/DNA complexes by anionic lipids. *Appl. Phys. Lett.* **2006**, *89*, 233903.